Science and Technology Indonesia
e-ISSN:2580-4391 *p*-ISSN:2580-4405
Vol. 10, No. 2, April 2025

Research Paper

Sonochemical Synthesis of Rutile Phase Copper-Doped Titanium Dioxide Coating on Fabric and Its Application in Antibacterial Testing of *Staphylococcus aureus*

Yi Bin Chew[1,2], Chui Min Ling[1], Pei Wen Koh[2], Chee Seng Chew[2], Siew Ling Lee[1,3*]

[1]*Department of Chemistry, Faculty of Science, Universiti Teknologi Malaysia, Johor Bahru, 81310, Malaysia*
[2]*CSC Screen Process Supplies Sdn Bhd, Johor Bahru, 81100, Malaysia*
[3]*Centre for Sustainable Nanomaterials, Ibnu Sina Institute for Scientific and Industrial Research, Universiti Teknologi Malaysia, Johor Bahru, 81310, Malaysia*
***Corresponding author**: lsling@utm.my

Abstract
In recent years, the utilization of copper-doped titanium dioxide (Cu-TiO_2) photocatalysts in antimicrobial activity has received intensive attention from researchers, especially during the COVID-19 pandemic. However, the common synthesis method of Cu-TiO_2 such as the sol-gel method would not be applicable in the industrial processes because of the low production yield of the photocatalysts. Besides, anatase TiO_2 is always arguable due to its high cost and less stable after a long synthesis process. Therefore, in this study, the sonochemical method was utilized to produce the Cu-TiO_2 photocatalysts using TiO_2 rutile as a precursor. The physicochemical properties of the synthesized photocatalysts were examined via several instrumental techniques. As evidenced by the X-ray diffraction (XRD) analysis, all the Cu-TiO_2 samples were formed in the rutile phase. Diffuse reflectance ultraviolet-visible (DRUV-Vis) analysis results indicated the wavelength extension to the visible region upon Cu loading. The antibacterial properties of Cu-TiO_2 photocatalysts were assessed via antibacterial testing using the Gram-positive bacteria, *Staphylococcus aureus*. The results indicated that the 5 mol% Cu-TiO_2 achieved the highest antibacterial efficiency of 75.8% under visible light irradiation for 1 hour. The current findings suggest that the Cu-TiO_2 photocatalysts could be produced via a straightforward and cost-effective synthesis method, which may continue with large-scale production and for application as an antimicrobial agent.

Keywords
Sonochemical, Fabric Coating, Antibacterial, Copper Dopant, Rutile-Phase Titanium Dioxide

Received: 1 July 2024, Accepted: 18 October 2024
https://doi.org/10.26554/sti.2025.10.2.605-613

1. INTRODUCTION

Pathogenic microorganisms in the surroundings cause severe outcomes and risks to human health because they could be transmitted directly from close contact with people or indirectly such as contamination of the surface when enclosed in the environment of pathogenic microorganisms. Amidst the COVID-19 pandemic, the usages of biocides have captured a lot of attention for their antimicrobial properties because pathogenic microbes may induce both healthcare-acquired infections (HAIs) and community-acquired infections (CAIs) (Salah et al., 2021). The utilization of metal oxides as antibacterial agents was discovered and studied in recent years because of the physiochemical and photochemical properties of metal oxides as photocatalysts. The metal oxide photocatalysts would not promote the resistance of bacteria and thus exhibit great safety from the inhibition of bacteria. Furthermore, the metal oxide photocatalysts including zinc oxide and argentum oxide demonstrated significant photochemical efficiency in antibacterial applications as a result of a broad spectrum of light absorption from UV to near-infrared light (Ma et al., 2024).

Titanium dioxide (TiO_2) has been well-known as a photocatalyst for a few decades due to its non-toxicity, high chemical stability, cost-friendly and excellent photocatalytic performance of TiO_2 (Koh et al., 2017, 2020). With its outstanding photochemical properties, TiO_2 could be utilized in the application of purification, disinfection, degradation, and self-cleaning which might be employed in places with high-risk HAIs and CAIs such as hospitals, clinics, and even communities (Margaretta et al., 2019). Although both rutile and anatase TiO_2 exhibited significant photocatalytic properties and bacterial reduction, they show low sensitivity to visible light (Saravanan et al., 2021). As a result, the generation of reactive oxygen species (ROS) important for microbial killing could only be done by TiO_2 in the presence of artificial UV light. Therefore, the metal doping on TiO_2's surface appears crucial to enhance the photochemical properties of TiO_2 under visible light and solar light. This is due to the surface plasmon resonance (SPR)

effects between the metal dopant and TiO_2 which could improve the photocatalytic antibacterial efficiency of TiO_2 under the irradiation of visible light and solar light (Leong et al., 2023).

Among all the transition metals, copper (Cu) is an excellent metal as the photocatalyst modifier and antimicrobial agent due to the high activity under visible light region and high bacterial killing efficiency (BKE) within a short time. A previous study reported that the BKE of Cu reached up to 99.99% within the contact time of two hours only (Montero et al., 2019). Besides, Cu nanoparticles can be applied as a coating to treat the pathogenic microbes in the environment. Therefore, Cu could be a suitable dopant for TiO_2 for antimicrobial activity under visible light illumination. Recently, Cu-doped TiO_2 was prepared via the micro-arc oxidation method (Tang et al., 2024). As reported, the bacterial reduction efficiency of copper-doped anatase TiO_2 was higher compared to the pure TiO_2 under visible light irradiation. Hence, it can be seen that the copper dopant on TiO_2 could activate the visible light absorption efficiency of the composite, improving the bacterial reduction efficiency (Tang et al., 2024). However, the copper oxide dopant ratio on TiO_2 should be optimized because a higher dopant ratio of copper oxide on TiO_2 could lead to faster electron and hole recombination and block active sites on the TiO_2 surface. The excess copper oxide dopant would also agglomerate on the TiO_2 surface and hence inhibit the visible light penetration, thus reducing the photocatalytic activity (Qaderi et al., 2021).

There are various methods and treatments for the synthesis of TiO_2 and TiO_2-based photocatalysts such as sol-gel, wet-impregnation, deposition, physical mixing, hydro/solvothermal, and sonochemical methods (Aslam et al., 2021; Koh et al., 2019). The great tunability and ability to produce nanoscale particles of TiO_2 could be the beneficial advantages of conventional synthesis methods such as the sol-gel and hydrothermal-solvothermal methods (Jassal et al., 2022). However, there are also some drawbacks to using the conventional synthesis methods. For instance, the sol-gel method requires expensive raw materials and high drying and calcination temperatures, which may lead to high consumption of energy and synthesis time (Alabdallah et al., 2024). Furthermore, hydrothermal treatment involves high temperature and high pressure during the synthesis process, long synthesis time, and the inability to control crystallinity (Jarusheh et al., 2022)). Therefore, sonochemical treatment appears as a suitable method for TiO_2 nanoparticle synthesis. This is due to the ease of controlling the morphology of TiO_2, short synthesis time, and favorable synthesis conditions such as room temperature (Chen et al., 2019)).

This paper presents the synthesis of rutile phase Cu-TiO_2 photocatalysts using the sonochemical method. In this work, a series of Cu-TiO_2 photocatalysts of different Cu dopant amounts (0 – 10 mol%) was synthesized using rutile TiO_2, a cheaper commercial TiO_2 as a precursor. The antibacterial performance of the synthesized photocatalysts coated on fabric was assessed through the antibacterial testing of a gram-positive bacteria, *Staphylococcus aureus*. Using *Staphylococcus aureus* in antibacterial testing with Cu-TiO_2 photocatalysts is crucial because it is recognized as a major human pathogen that causes a wide range of infections, from mild skin infections to severe systemic diseases. Testing against *S. aureus* is highly relevant for public health because it provides insights into the potential applications of Cu-TiO_2 for combating Gram-positive bacterial infections, which are generally harder to kill. This is because Gram-positive bacteria have a thicker peptidoglycan layer that offers more resistance to reactive oxygen species (ROS) generated by photocatalysts compared to Gram-negative bacteria. Therefore, it is widely accepted that a material may possess strong antibacterial properties and broader applicability if it can effectively kill *Staphylococcus aureus* (Aravind et al., 2021).

2. EXPERIMENTAL SECTION

2.1 Materials

Rutile TiO_2 (TR595, 99%) was purchased from Crystal Company. Meanwhile, copper(II) nitrate ($Cu(NO_3)_2$, 99%), sodium hydroxide (NaOH), and ethylene glycol ($C_2H_6O_2$, 99%) were acquired from Merck Chemical Company.

2.2 Photocatalyst Preparation

A series of Cu-TiO_2 photocatalysts was produced with different loading amounts of Cu dopants ranging from 1 to 10 mol%. The photocatalysts were synthesized via the sonochemical method. TiO_2 dispersion (undoped TiO_2) was prepared for the comparison purpose. All the photocatalysts were produced using the chemicals without prior purification.

Preparation of Cu-TiO_2 Cu-TiO_2 was synthesized via the sonochemical approach as described elsewhere with minor modification (Jhuang and Cheng, 2016). Firstly, the rutile TiO_2 powder was dissolved in a solution containing NaOH and $C_2H_6O_2$. The mixture was labeled as Mixture X. Next, 1 mol% $Cu(NO_3)_2$ was added into Mixture X. After that, the resulting mixture was sonicated for 15 minutes to complete the synthesis procedure. In this work, a series of Cu-TiO_2 samples of the different $Cu(NO_3)_2$ doping amounts, ranging from 1 to 10 mol%, was synthesized.

2.3 Characterization of Photocatalysts

The physicochemical properties of the TiO_2 dispersion and the prepared Cu-TiO_2 photocatalysts were investigated. The particle size and distribution of the synthesized photocatalysts were determined using Malvern Zetasizer Nano ZS with dynamic light scattering. The rheological information of the synthesized photocatalysts was obtained via the rotational modes using the Anton Paar Modular Compact Rheometer, MCR 302. The color appearance and opacity of the as-prepared photocatalysts were identified by the Datacolor 800 color spectrometer.

The powder X-ray diffraction (XRD) analysis via the Rigaku SmartLab was employed to determine the crystallinity and molecular structure of the photocatalysts. The chemical states and element composition of the synthesized photocatalysts were examined using X-ray photoelectron spectroscopy via the

Kratos XPS Axis. The light absorption capability of the photocatalysts was studied via diffuse reflectance ultraviolet-visible (DR UV-Vis) analysis using Shimadzu UV-3600 Plus Spectrometer. The morphology of the synthesized samples was examined by field emission scanning electron microscopy (FE-SEM) using the JEOL FESEM with the model JSM-6701F, while the elemental analysis was conducted by the Energy Dispersive X-ray (EDX) analysis.

2.4 Coating of Copper-Doped Titania on Polyester Fabric

The as-synthesized copper-doped TiO_2 was added into an acrylic base textile screen printing paste to apply on polyester mask fabric before the antibacterial testing using the AATCC TM 100 test method. Firstly, 5% of each molar ratio of copper-doped TiO_2 was dispersed into the acrylic base textile screen printing ink. Later, the prepared mixture was coated on the fabric via the screen print method using the TAS Compact CX12 Textile Screen Printing machine.

2.5 Antimicrobial Testing

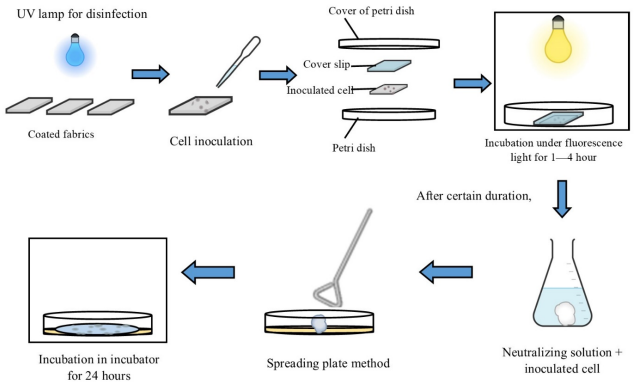

Figure 1. Schematic Diagram Showing Antimicrobial Testing Using Coated Fabric

The schematic diagram for antimicrobial testing using coated fabric is illustrated in Figure 1. The antimicrobial performance of the synthesized materials coated on fabric was evaluated using Staphylococcus aureus bacteria under 1000 lux of fluorescent daylight. In brief, Staphylococcus aureus was seeded onto the coated fabric, and then covered with a sterilized glass slip. After that, the incubation of bacteria on the coated fabrics was conducted under the fluorescent light at a light intensity of 1000 lux for 10 – 240 minutes. Following the neutralization of the bacteria using Dey-Engley neutralizer, the spread plate method was employed to enumerate them. The reduction percentage in bacteria was calculated using Equation 1:

$$\frac{(C-A)}{C} \times 100\% = R \quad (1)$$

Where R is the reduction percentage, C refers to the number of bacteria recovered from the inoculated treated test specimen swatches in the jar immediately after inoculation (at a contact time of 0) and A represents the number of bacteria recovered from the inoculated treated test specimen swatches in the jar incubated over predetermined contact time (at a contact time of t min).

3. RESULT AND DISCUSSION

3.1 Structural Study

3.1.1 Particle Size and Zeta Potential Analysis

The particle size and zeta potential for the undoped rutile TiO_2 and Cu-TiO_2 are exhibited in Figure 2 (a). As shown, the particle size of undoped TiO_2 was roughly 234 nm and the particle size increased significantly by 46% after the incorporation of 1 mol% Cu into TiO_2 (342 nm). However, the introduction of more Cu dopants into TiO_2 had no obvious change in the particle size as other Cu-TiO_2 samples have particle sizes ranging from 302 – 320 nm. The results are a good indication of the successful doping of Cu ions in the TiO_2 lattice which the presence of the dopant ions has induced the aggregation or growth of TiO_2 particles (Leong et al., 2022).

On the other hand, the zeta potential analysis exhibited a significant increment from -19.47 mV for undoped TiO_2 to positive values as high as 42.87 mV for the Cu-TiO_2 samples. The increase of zeta potential strongly suggests the improvement in colloidal stability which is associated with the samples' surface charge after the Cu doping. As evidenced, the particles' surface of all the Cu-TiO_2 samples are positively charged, thereby preventing aggregation (Pinton and Bulhões, 2019). This material property is particularly advantageous when applying the particles in suspensions, such as painters, coaters, and photocatalysts.

The polydispersity indexes (PDI) of undoped TiO_2 and Cu-TiO_2 are illustrated in Figure 2 (b). All the synthesized Cu-TiO_2 samples have low to moderate PDI values ranging from 0.12 to 0.20, corresponding to the uniform and narrow particle size distribution and good stability even after the Cu doping (Takechi-Haraya et al., 2022). The findings implied that the Cu doping process did not cause significant heterogeneity in particle size.

3.1.2 X-Ray Diffraction (XRD) Analysis

Figure 3 shows the XRD patterns of undoped TiO_2 and Cu-TiO_2 samples. As expected, the XRD pattern of the undoped TiO_2 samples displayed the sharp peaks at 2θ = 27.4°, 36.1°, 41.2°, 54.3°, 56.6°, and 69.0°, which indicated the single phase of rutile TiO_2 attainment (Phromma et al., 2020). The sharp and intense peaks indicate the high crystallinity and well-ordered structure of the TiO_2 sample. Meanwhile, the XRD patterns of Cu-TiO_2 samples are identical to those of undoped TiO_2, without any significant shifting of the primary peaks of the rutile phase after the sonochemical synthesis process. Peaks corresponding to Cu dopant were not detected even in the 10 mol% Cu-doped TiO_2 sample, indicating that the loading of Cu

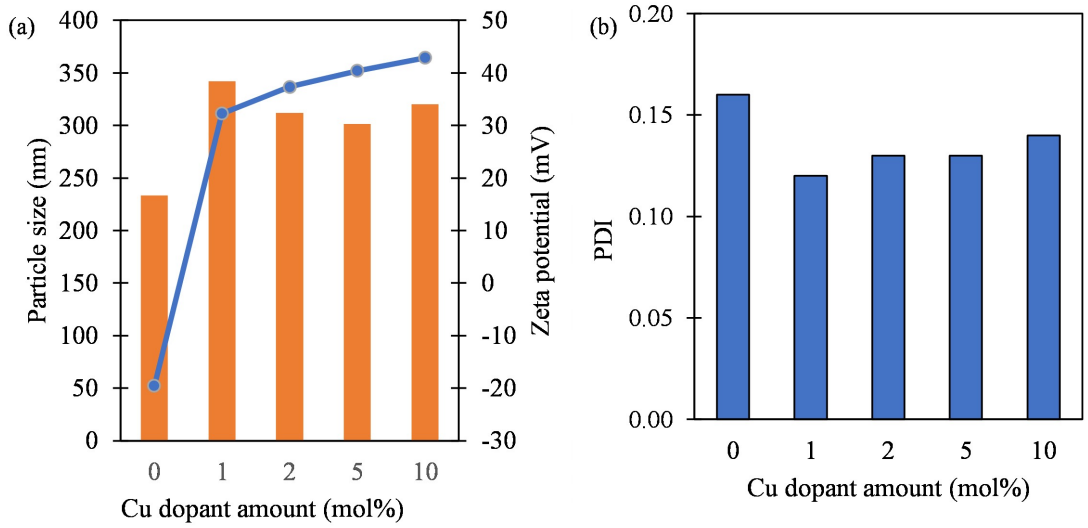

Figure 2. (a) Particle Size and Zeta Potential of Rutile TiO_2 and Cu-TiO_2 Samples; (b) Polydispersity Indexes of Rutile TiO_2 and Cu-TiO_2 Samples

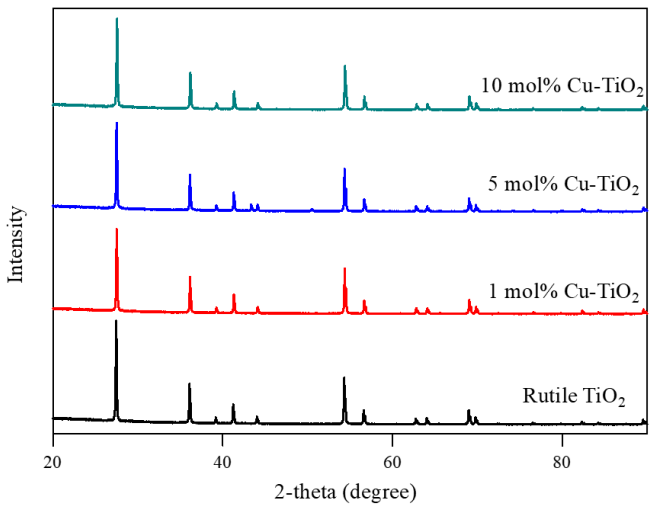

Figure 3. XRD Patterns of Rutile TiO_2 and Cu-TiO_2 Samples

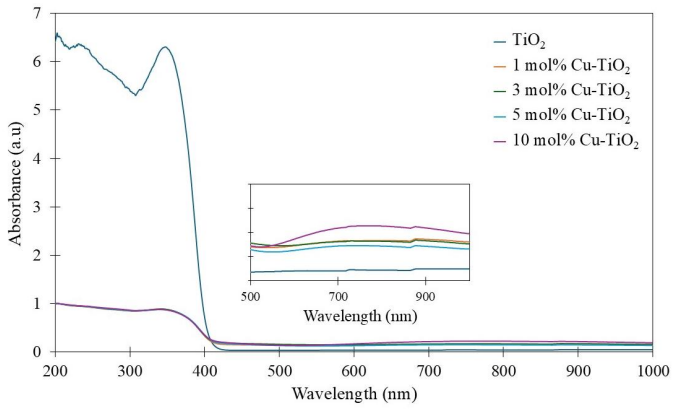

Figure 4. DR UV-Vis Spectra of Rutile TiO_2 and Cu-TiO_2 Samples

ions into the TiO_2 did not affect the crystal structure of TiO_2 (Chen et al., 2019; Mathew et al., 2018). As can be seen, the presence of Cu dopant has slightly decreased the crystallinity of the samples. This could be indirect evidence of the successful loading of Cu ions into the TiO_2 lattice (Ahmadiasl et al., 2022). The XRD results confirmed that the rutile phase of TiO_2 remained after Cu doping via the sonochemical process.

3.2 Optical Study

The diffuse reflectance UV-Vis (DRUV-Vis) spectra of the undoped TiO_2 and Cu-TiO_2 samples are illustrated in Figure 4. The absorption edge of the undoped TiO_2 was present at 400 nm, which indicated the presence of peroxo-titanium complexes in the undoped TiO_2 representing the excitation of electrons from the valence band to the conduction band within TiO_2 particles (Park et al., 2022). The absorption peak at around 350 nm could be indicative of the dominant octahedrally coordinated Ti species in the sample.

All the Cu-TiO_2 samples displayed similar absorption edges at around 420 nm (Figure 4). As shown, all the Cu-TiO_2 samples exhibited slight redshifts to the visible light region at higher wavelengths, correlating to the minor reduction in the band gap energy from 3.10 (for undoped TiO_2) to 2.95 eV after the successful incorporation of Cu dopant into the TiO_2 lattice, introducing localized states within the band gap of TiO_2 (Adamu et al., 2023). As shown in the inserted figure, a slight increment in absorbance in the visible light region at 500 – 1000 nm was observed for all the Cu-TiO_2 samples. The

intensity of the absorbance at around 750 nm increased with the increase of Cu dopant amount, implying the Cu dopant in the samples induced the new electronic states within the conduction band and valence band of TiO_2 and thus enhancing the absorptivity of the materials toward visible light (Leong et al., 2022).

3.3 Elemental Analysis

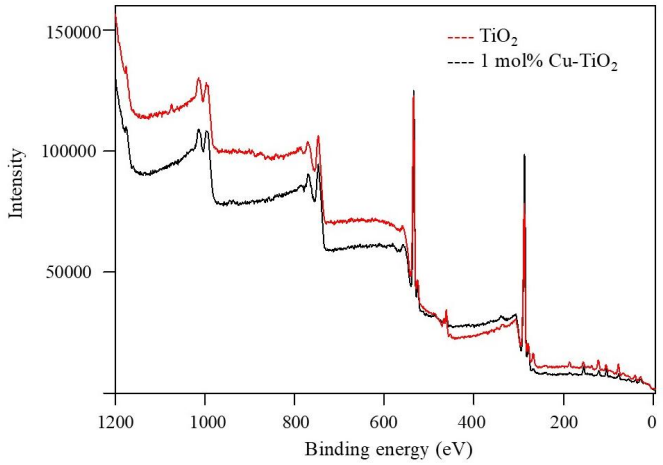

Figure 5. X-Ray Photoelectron Spectra of Undoped TiO_2 and 1 mol% Cu-TiO_2

The elemental compositions and chemical states of undoped TiO_2 and copper-doped TiO_2 were determined using X-ray photoelectron spectroscopy (XPS) analysis. The results displayed in Figure 5 showed that the undoped TiO_2 exhibited distinct peaks of titanium and oxygen, with binding energies correlating to the Ti 2p and O 1s peaks. The Ti 2p 3/2 peak and the O 1s peak were observed at around 458.5 eV and approximately 530.1 eV, respectively. It was indicated that the stoichiometric composition of undoped TiO_2 was compatible with previous studies (El Nemr et al., 2019). For Cu-TiO_2 materials, any obvious peaks corresponding to copper ions were not detected particularly the Cu 2p 3/2 peak at around 932.6 eV, which indicated the low concentration of copper element on the surface of TiO_2. Besides, the low concentration of copper element on TiO_2 was beyond the limit of detection (LOD) of the XPS instrument.

There is no significant shifting in binding energies for the Ti 2p and O 1s peaks for the copper-doped TiO_2 compared to undoped TiO_2. The Ti 2p 3/2 peak was approximately 458.5 eV, and the O 1s peak was around 530.1 eV. This is due to the insignificant alteration of the electronic environment between the Ti and O atoms after Cu doping, thus indicating no substantial change in the TiO_2 lattice structure after the Cu doping or no formation of Ti−O−Cu bonds (Temperton et al., 2019). Copper was likely incorporated into the TiO_2 nanoparticles in some form, even if it was not detected by XPS due to detection limits imposed by the XPS, considering the process conditions and intended doping levels.

3.4 Morphological Study

The morphology properties and elemental analysis of undoped TiO_2 and Cu-TiO_2 were investigated by the FESEM and EDX mapping. The FESEM images shown in Figure 6 (a) and (b) reveal that the undoped TiO_2 exhibited a uniform and consistent spherical morphology and smooth surfaces. This may be due to the high degree of uniformity during the synthesis of TiO_2. Conversely, 1 mol% Cu-TiO_2 exhibited some aggregation and irregular shapes in its morphology. This indicated the successful loading of copper dopant on TiO_2 which altered the morphology and formed the particles with different sizes and shapes (Raguram and Rajni, 2019).

The EDX mapping analysis of the undoped TiO_2 and Cu-TiO_2 are illustrated in Figure 6 (c) and (d). For the undoped TiO_2, the presence of titanium and oxygen in uniform distribution was detected, corresponding to the expected stoichiometry of TiO_2. For 1 mol% Cu-TiO_2, it showed that the Cu dopant present in localized space within the TiO_2 matrix (Raguram and Rajni, 2019). Despite the relatively uniform distribution of Cu, the signals were not as strong as expected, possibly due to the detection limit of the instrument. Alternatively, a slight loss of Cu might have happened during the sample drying process. The FESEM and EDX mapping results indicated that Cu doping altered the morphology and elemental composition of the samples. As a result of this incorporation, the electronic and surface properties of the nanoparticles might be modified, which could enhance their functionality for various applications, including photocatalysis and environmental remediation.

3.5 Rheology and Appearance Studies

3.5.1 Rheology of Cu-TiO_2 Mixed with Textile Screen Printing Ink

The rheology of the prepared materials was determined via Anton Paar Modular Compact Rheometer MCR302, and the graph of viscosity against shear rate is shown in Figure 7. As can be seen, 1 mol% Cu-TiO_2, 3 mol% Cu-TiO_2, and 5 mol% Cu-TiO_2 samples exhibited similar pseudoplastic flow characteristics after mixing copper-doped titania with textile screen printing ink. However, the initial viscosity of 10 mol% Cu-TiO_2 was relatively lower as compared to the other samples. This may be due to the low pH of the sample, which has rendered it incompatible with acrylic-based textile screen printing ink (Jawad and Jassim, 2020). A significant reduction in the viscosity of the ink paste could lead to a decrease in binding strength on the substrate, resulting in poor fastness and lower durability. Consequently, due to the low pH, 10 mol% Cu-TiO_2 and higher Cu-loaded samples would not be suitable for printing applications as the viscosity of the samples would have reduced to an unacceptable level. As for the remaining Cu-TiO_2 samples including 1 mol% Cu-TiO_2, 3 mol% Cu-TiO_2, and 5 mol% Cu-TiO_2 samples that possessed adequate pseudoplastic properties, they were suitable for application and tested for antimicrobial activity with AATCC TM 100.

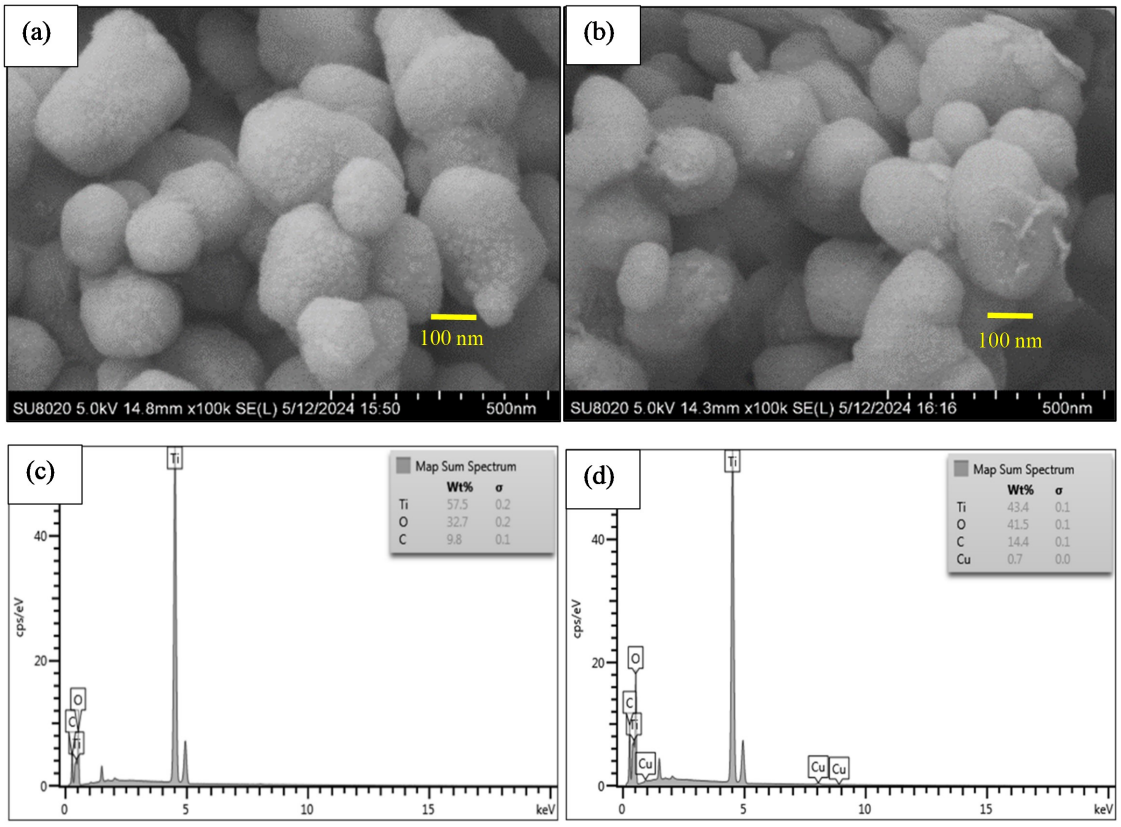

Figure 6. (a) FESEM Image of Undoped Rutile TiO_2, (b) FESEM Image of 1 mol% Cu-TiO_2, (c) EDX Elemental Analysis for Undoped TiO_2, (d) EDX Elemental Analysis for 1 mol% Cu-TiO_2

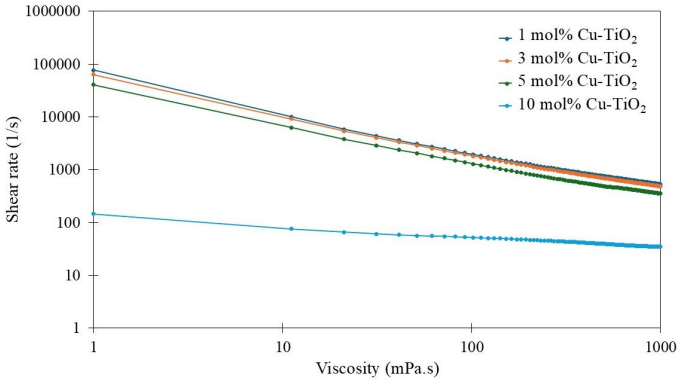

Figure 7. Graph of Shear Rate Against Viscosity of Cu-TiO_2 Samples

3.5.2 Appearance of Cu-TiO_2 Mixed Textile Screen Print Ink

All the acceptable samples were coated onto a Form 2A opacity chart and the color values (CIE L, CIE a, CIE b, and opacity) were investigated and are tabulated in Table 2. As Cu content increased, the values of CIE L and CIE a of the samples decreased, while CIE b values slightly changed. Besides, the opacity values increased with the increase of the Cu dopant amount in the samples. The decrease of values in CIE L and CIE a could be associated with the decrease of whiteness and increase in bluishness of the samples. The sample appeared bluer as Cu dopant content in Cu-TiO_2 increased, indicative of the successful loading of Cu in the samples. Notably, 10 mol% Cu-TiO_2 was not assessed for the color value test as its viscosity was not compatible with the textile screen printing method. The viscosity of 10 mol% Cu-TiO_2 was too low to achieve proper ink transfer and uniform coverage during the textile screen printing process. Such low viscosity results in poor adhesion and inconsistent application on the fabric, making it unsuitable for producing reliable and repeatable color measurements.

Table 1. Colour Value Measurement of Cu-TiO_2 Mixed Textile Screen Print Ink

Sample	CIE L	CIE a	CIE b	Opacity
1 mol% Cu-TiO_2	93.05	-0.65	2.95	30.18
2 mol% Cu-TiO_2	92.88	-1.09	2.83	33.25
5 mol% Cu-TiO_2	92.26	-2.68	2.91	34.78

3.6 Antimicrobial Testing of Cu-TiO_2

The antibacterial testing of all the samples was conducted via the standard test method, AATCC TM100-2019 – Test Method for Antibacterial Finishes on Textile Materials: Assessment. The antibacterial performance of Cu-TiO_2 coated on fabric was assessed using gram-positive bacteria, Staphylococcus aureus, and light exposure of 1000 lux of fluorescent lamp during inoculation of bacteria. The bacteria-killing efficiencies (BKE) of all the samples of Cu-TiO_2 are tabulated in Table 2.

Table 2. Bacteria Killing Efficiency (BKE) of Cu-TiO_2 Catalysts Under Dark and Visible Light Irradiation for 1 hour Reaction Time

Sample	Bacterial killing efficiency (%)	
	Dark	Visible Light
Rutile TiO_2	30.6	31.5
1 mol% Cu-TiO_2	38.7	46.8
2 mol% Cu-TiO_2	55.7	62.9
5 mol% Cu-TiO_2	49.0	75.8

The experimental data revealed that rutile TiO_2 exhibited 30.6% BKE under dark condition. It is not surprising as rutile TiO_2 has been documented as a good antibacterial coating material (Rajput and Kale, 2023). The BKE of TiO_2 increased after Cu doping. Amongst, 2 mol% Cu-TiO_2 showed the highest BKE of 55.7% with an increment about 2-fold under the same reaction condition, indicating the optimum amount of Cu dopant is important for the synergetic effect of Cu-TiO_2 in enhancing the antibacterial activity. As reported previously, the Cu dopant was able to spread and hence improved the antibacterial activity by releasing Cu ions, resulting in effective antibacterial activity against *S. aureus* (Kayani et al., 2022).

Under visible light irradiation, the BKE of rutile TiO_2 slightly increased to 31.5%. Since a wavelength filter was not used during the reaction, it is believed that the TiO_2 was activated by the minimal ultraviolet light from the light source, resulting in the generation of hydroxyl radicals (·OH) and superoxide anion ($\cdot O^{2-}$) radicals (Mathew et al., 2018). All the Cu-doped samples have higher BKE than that of rutile TiO_2 under visible light irradiation. The improvement could be due to the reduced band gap energy and the absorption at visible light region upon Cu doping, as evidenced by the DR UV-Vis analysis. The improved properties in Cu-TiO_2 samples have facilitated the generation of more radicals which play an important role in damaging the bacterial membrane, causing cell death. Besides, it was reported previously that the Cu dopant might have acted as an electron scavenger, bringing into a slower electron-hole recombination rate and hence increasing the amount of the radicals for bacterial killing.

Sample 5 mol% Cu-TiO_2 recorded the highest BKE of 75.8% under visible light irradiation for 1 h. The experiment data showed that the sample achieved > 99% BKE after a reaction time of 4 h. The current findings indicated that the synthesized Cu-TiO_2 samples were effective antibacterial agents under both dark and visible light.

4. CONCLUSIONS

A series of Cu-TiO_2 of different mol% Cu dopants, ranging from 1 to 10 mol%, were synthesized using rutile TiO_2 as a precursor via a sonochemical method. The analysis data confirmed that the particle size of the resulting materials ranged from 230 – 350 nm. All the samples were crystallized solely in the rutile phase. The antibacterial properties of copper-doped titania photocatalysts were assessed via antibacterial testing using the Gram-positive bacteria, Staphylococcus aureus under both dark and visible light irradiation. It has been demonstrated the synthesized Cu-TiO_2 were good visible-light-driven photocatalysts for antibacterial. Due to its enhanced structural and optical properties, the presence of Cu dopant has extended the light absorption range of TiO_2 into the visible light spectrum, significantly improved its photocatalytic efficiency, and hence increased the BKE of the samples. Sample 5 mol% Cu-TiO_2 achieved the highest BKE of 75.8% under visible light for 1 h. A cost-effective TiO_2 precursor and scalable synthesis method were highlighted in this work as an effective approach for creating functional materials that can address current technological, medical, and environmental challenges.

5. ACKNOWLEDGMENT

The authors acknowledge the financial support received from the Ministry of Higher Education Malaysia (MOHE) and Universiti Teknologi Malaysia (UTM) through the Potential Academic Staff grant (cost center: Q.J130000.2754.03K86). The authors are grateful to the University Industry Research Laboratory, UTM for the research facilities including XRD and FESEM-EDX.

REFERENCES

Adamu, A., M. Isaacs, K. Boodhoo, and F. R. Abegão (2023). Investigation of Cu/TiO_2 Synthesis Methods and Conditions for CO_2 Photocatalytic Reduction via Conversion of Bicarbonate/Carbonate to Formate. *Journal of CO_2 Utilization*, **70**; 102428

Ahmadiasl, R., G. Moussavi, S. Shekoohiyan, and F. Razavian (2022). Synthesis of Cu-Doped TiO_2 Nanocatalyst for the Enhanced Photocatalytic Degradation and Mineralization of Gabapentin Under UVA/LED Irradiation: Characterization and Photocatalytic Activity. *Catalysts*, **12**(11); 1310

Alabdallah, N. M., S. M. Alluqmani, H. M. Almarri, and A. A. AL-Zahrani (2024). Physical, Chemical, and Biological Routes of Synthetic Titanium Dioxide Nanoparticles and Their Crucial Role in Temperature Stress Tolerance in Plants. *Heliyon*, **10**(4); e26537

Aravind, M., M. Amalanathan, and M. M. M. Sony (2021). Synthesis of TiO_2 Nanoparticles by Chemical and Green Synthesis Methods and Their Multifaceted Properties. *SN Applied Sciences*, **3**; 409

Aslam, M., A. Z. Abdullah, and M. Rafatullah (2021). Recent Development in the Green Synthesis of Titanium Dioxide Nanoparticles Using Plant-Based Biomolecules for Environmental and Antimicrobial Applications. *Journal of Industrial and Engineering Chemistry*, **98**; 1–16

Chen, J., J. Yan, and G. Gan (2019). The Effect of Cu Doping on the Transformation from Rutile to Anatase and Cu Occupation Tendency in TiO_2 Solid Solution. *Journal of Spectroscopy*, **2019**(1); 6470601

El Nemr, A., E. Helmy, E. Gomaa, S. Eldafrawy, and M. Mousa (2019). Photocatalytic and Biological Activities of Undoped and Doped TiO_2 Prepared by Green Method for Water Treatment. *Journal of Environmental Chemical Engineering*, **7**(5); 103385

Jarusheh, H. S., A. Yusuf, F. Banat, M. A. Haija, and G. Palmisano (2022). Integrated Photocatalytic Technologies in Water Treatment Using Ferrites Nanoparticles. *Journal of Environmental Chemical Engineering*, **10**(5); 108204

Jassal, P. S., D. Kaur, R. Prasad, and J. Singh (2022). Green Synthesis of Titanium Dioxide Nanoparticles: Development and Applications. *Journal of Agriculture and Food Research*, **10**; 100361

Jawad, A. J. and A. E. Jassim (2020). Effect of Titanium Dioxide Nanoparticles (TiO_2 NPs) on Rheological Characteristics Behavior of Poly Vinyl Acetate (PVAc). *Nano World Journal*, **6**(3); 61–65

Jhuang, Y. and W. Cheng (2016). Fabrication and Characterization of Silver/Titanium Dioxide Composite Nanoparticles in Ethylene Glycol with Alkaline Solution Through Sonochemical Process. *Ultrasonics Sonochemistry*, **28**; 327–333

Kayani, Z. N., M. Ashfaq, S. Riaz, and S. Naseem (2022). Impact of Cu on Structural, Optical, Dielectric Properties and Antibacterial Activity of TiO_2 Thin Films. *Optical Materials*, **132**; 112809

Koh, P. W., M. H. M. Hatta, S. T. Ong, L. Yuliati, and S. L. Lee (2017). Photocatalytic Degradation of Photosensitizing and Non-Photosensitizing Dyes Over Chromium Doped Titania Photocatalysts Under Visible Light. *Journal of Photochemistry & Photobiology, A: Chemistry*, **332**; 215–223

Koh, P. W., C. Y. Leong, L. Yuliati, H. Nur, and S. L. Lee (2020). Role of Vanadia and Titania Phases in the Removal of Methylene Blue by Adsorption and Photocatalytic Degradation. *Malaysian Journal of Analytical Sciences*, **24**(6); 1045–1060

Koh, P. W., L. Yuliati, and S. L. Lee (2019). Kinetics and Optimization Studies of Photocatalytic Degradation of Methylene Blue Over Cr-Doped TiO_2 Using Response Surface Methodology. *Iran Journal of Science and Technology, Transactions A: Science*, **43**(1); 95–103

Leong, C. Y., H. L. Teh, M. C. Chen, and S. L. Lee (2022). Effect of Synthesis Methods on Properties of Copper Oxide Doped Titanium Dioxide Photocatalyst in Dye Photodegradation of Rhodamine B. *Science & Technology Indonesia*, **7**(1); 91–97

Leong, C. Y., R. A. Wahab, S. L. Lee, V. K. Ponnusamy, and Y.-H. Chen (2023). Current Perspectives of Metal-Based Nanomaterials as Photocatalytic Antimicrobial Agents and Their Therapeutic Modes of Action: A Review. *Environmental Research*, **227**; 115578

Ma, S., X. Li, J. Kong, X. Yu, and X. Bai (2024). Light-Triggered Bactericidal Semiconductor Nanomaterials: Classification, Modification and Antibacterial Strategies. *Applied Materials Today*, **39**; 102279

Margaretta, D. O., K. W. Permadi, D. Y. Rahman, F. D. Utami, S. Viridi, and M. Abdullah (2019). Antibacterial Investigation Activity of Titania Anatase Technical Grade on Polypropylene Sheet. *Journal of Physics: Conference Series*, **1204**; 012051

Mathew, S., P. Ganguly, S. Rhatigan, V. Kumaravel, C. Byrne, S. Hinder, and E. McKenna (2018). Cu-Doped TiO_2: Visible Light Assisted Photocatalytic Antimicrobial Activity. *Applied Sciences*, **8**(11); 2067

Montero, D. A., C. Arellano, M. Pardo, R. Vera, R. Gálvez, M. Cifuentes, and R. M. Vidal (2019). Antimicrobial Properties of a Novel Copper-Based Composite Coating with Potential for Use in Healthcare Facilities. *Antimicrobial Resistance & Infection Control*, **8**(3); 1–10

Park, H., D. H. Han, T. Goto, S. Cho, Y. Morimoto, and T. Sekino (2022). A Facile Bottom-Up Method for Synthesis of Peroxo-Potassium Titanate Nanoribbons and Visible Light Photocatalytic Activity Derived from a Peroxo-Titanium Bond. *Nanoscale Advances*, **4**; 3573

Phromma, S., T. Wutikhun, P. Kasamechonchung, T. Eksangsri, and C. Sapcharoenkun (2020). Effect of Calcination Temperature on Photocatalytic Activity of Synthesized TiO2 Nanoparticles via Wet Ball Milling Sol-Gel Method. *Applied Sciences*, **10**(3); 993

Pinton, A. P. and L. O. S. Bulhões (2019). Synthesis, Characterization, and Photostability of Manganese-Doped Titanium Dioxide Nanoparticles and the Effect of Manganese Content. *Materials Research Express*, **6**; 125015

Qaderi, J., C. R. Mamat, and A. A. Jalil (2021). Preparation and Characterization of Copper, Iron, and Nickel Doped Titanium Dioxide Photocatalysts for Decolorization of Methylene Blue. *Sains Malaysiana*, **50**(1); 135–149

Raguram, T. and K. S. Rajni (2019). Synthesis and Analysing the Structural, Optical, Morphological, Photocatalytic and Magnetic Properties of TiO_2 and Doped (Ni and Cu) TiO_2 Nanoparticles by Sol–Gel Technique. *Applied Physics A*, **125**; 288

Rajput, R. B. and R. B. Kale (2023). Photocatalytic Activity of Solvothermally Synthesized Rutile TiO_2 Nanorods for the Removal of Water Contaminants. *Journal of Environmental Chemical Engineering*, **11**(1); 109581

Salah, I., I. P. Parkin, and E. Allan (2021). Copper as an Antimicrobial Agent: Recent Advances. *RSC Advances*, **11**; 18179–18186

Saravanan, A., P. S. Kumar, S. Jeevanantham, S. Karishma, and A. R. Kiruthika (2021). Photocatalytic Disinfection of Micro-Organisms: Mechanisms and Applications. *Environmental*

Technology & Innovation, **24**; 101909
Takechi-Haraya, Y., T. Ohgita, Y. Demizu, H. Saito, K. I. Izutsu, and K. Sakai-Kato (2022). Current Status and Challenges of Analytical Methods for Evaluation of Size and Surface Modification of Nanoparticle-Based Drug Formulations. *AAPS PharmSciTech*, **23**; 150
Tang, J., F. Wei, L. Zhao, L. Yang, J. Li, Z. Sun, and B. Liu (2024). Superior Antibacterial Properties of Copper-Doped Titanium Oxide Films Prepared by Micro-Arc Oxidation. *Ceramics International*, **50**(1, Part B); 1370–1378
Temperton, R. H., A. Gibson, and J. N. O'Shea (2019). In Situ XPS Analysis of the Atomic Layer Deposition of Aluminium Oxide on Titanium Dioxide. *Physical Chemistry Chemical Physics*, **21**(3); 1393–1398